C. R. Physique 16 (2015) 368–378

Contents lists available at ScienceDirect

Comptes Rendus Physique

www.sciencedirect.com

Highlights of the LHC run 1 / Résultats marquants de la première période d'exploitation du GCH

Standard Model theory calculations and experimental tests

Calculs théoriques et tests expérimentaux du modèle standard

Matteo Cacciari [a], Gautier Hamel de Monchenault [b,*]

[a] *LPTHE, Paris, France*
[b] *CEA Saclay, Irfu–SPP, Gif-sur-Yvette, France*

ARTICLE INFO

Article history:
Available online 14 May 2015

Keywords:
LHC
CERN
ATLAS
CMS
Standard Model
Perturbative calculations

Mots-clés :
LHC
CERN
ATLAS
CMS
Modèle standard
Calculs perturbatifs

ABSTRACT

To present knowledge, all the physics at the Large Hadron Collider (LHC) can be described in the framework of the Standard Model (SM) of particle physics. Indeed the newly discovered Higgs boson with a mass close to 125 GeV seems to confirm the predictions of the SM. Thus, besides looking for direct manifestations of the physics beyond the SM, one of the primary missions of the LHC is to perform ever more stringent tests of the SM. This requires not only improved theoretical developments to produce testable predictions and provide experiments with reliable event generators, but also sophisticated analyses techniques to overcome the formidable experimental environment of the LHC and perform precision measurements. The present article proposes an overview of the present theoretical tools and of the experimental results in the field of strong and electroweak interactions.

RÉSUMÉ

À ce jour, l'ensemble de la physique du Grand collisionneur de hadrons LHC s'inscrit dans le cadre du modèle standard (MS) de la physique des particules. Ainsi la découverte récente du boson de Higgs avec une masse proche de 125 GeV confirme-t-elle une prédiction centrale du MS. L'une des missions principales du LHC, avec la recherche de manifestations directes de nouvelle physique au-delà du MS, consiste à soumettre le MS à des tests toujours plus contraignants. Cela requiert non seulement des outils théoriques toujours plus performants permettant des prédictions vérifiables et fournissant aux expériences des générateurs d'événements fiables, mais aussi des techniques d'analyse des données sophistiquées pour surmonter les conditions dantesques de l'environnement expérimental au LHC et permettre des mesures de précision. Cet article propose une vue d'ensemble des outils théoriques disponibles et des résultats expérimentaux récents dans le domaine des interactions fortes et électrofaibles.

* Corresponding author.
E-mail addresses: cacciari@lpthe.jussieu.fr (M. Cacciari), gautier.hamel-de-monchenault@cea.fr (G. Hamel de Monchenault).

http://dx.doi.org/10.1016/j.crhy.2015.04.004
1631-0705/

The standard model (SM) of particle physics has been (and, somewhat unfortunately, still is) enormously successful in describing experimental measurements in particle physics. Not only the last missing piece, the Higgs boson, has recently been observed [1,2], but all comparisons between measured and predicted cross sections at the Large Hadron Collider confirm the excellent agreement between theory and experiment already observed at older and less powerful colliders. While the LHC presents an unprecedented potential for the discovery of new phenomena beyond the SM (BSM), it is also of utmost importance to understand the SM processes, which constitute possible backgrounds to BSM signals. A variety of studies on SM processes are performed at the LHC, ranging from quantum chromodynamics (QCD) measurements to measurements with photons, leptons and vector bosons.

In the first Section, we describe the state of the art of the theoretical tools and event generators that are used to provide predictions for the production cross sections of the processes of interest. In Section 2, inclusive cross section measurements with jets, leptons and vector bosons are presented. Examples of differential cross sections, charge asymmetries and the study of lepton pairs are proposed in Section 3. Finally, in Section 4, we report studies on the multiple production of gauge bosons and constraints on anomalous gauge couplings.

1. Theoretical tools

The backbone of theoretical predictions for collider physics is represented by perturbative calculations in a Quantum Field Theory (QFT) context, i.e. power expansions in the (running) coupling of a renormalizable field theory. Such calculations are usually labeled by the highest power of the coupling at which they are known (e.g., $\alpha_s^2, \alpha_s^3, \ldots$) or by the relevance of the last known perturbative order (e.g., leading order (LO), next-to-leading order (NLO), next-to-next-to-leading order (NNLO), etc). A more complex labeling is needed when certain classes of terms are resummed to all orders. In this case, one may denote the resummation as being at "leading logarithmic" (LL) level, "next-to-leading logarithmic" (NLL), etc. Theoretical predictions that merge a fixed-order calculation with a resumed one can be labeled as "NLO–NLL", "NLO–NNLL", etc.

In many cases, "leading order" is synonymous with "tree level" or "Born approximation": the Feynman diagrams that contribute to the calculation of an observable at leading order are only of "tree" type, i.e. without closed loops.[1] Conversely, diagrams containing single loops often contribute to "next-to-leading" terms, double loops to "next-to-next-to-leading" ones, etc.

Calculation of tree diagrams in the SM was pioneered in the 1970s and the 1980s, and has long been considered a solved problem. Automation of these calculations (generation of relevant diagrams, calculation and squaring of the amplitudes, integration over the phase space) has similarly been available since a long time.

Tree-level calculations cannot usually provide a better-than-an-order-of-magnitude accuracy in predictions. For more than twenty years, from the 1980s until the early 2000s, the workhorse of phenomenological predictions for SM processes in collider physics has been constituted of (1) NLO calculations laboriously performed by hand one specific process at a time, a single calculation usually taking at least several months to complete; (2) LL resummations of emission of radiation in the soft and collinear limit, often available analytically but more usually implemented numerically in parton shower (PS) Monte Carlo event generators on top of leading order processes; (3) NLL resummations of selected classes of logarithms, usually calculated analytically and for specific processes.[2]

This long-standing state of the art has been upended, starting in the early 2000s, by a series of theoretical advances:

- the ability to match an NLO calculation with a parton shower Monte Carlo. This allows one to generate fully exclusive distributions for realistic events that, when integrated, retain NLO accuracy for production rates. It was first achieved in MC@NLO [3] and soon thereafter through the POWHEG [4] approach;
- new techniques for calculating complex loop integrals have allowed for the rapid proliferation of NLO calculation of multi-jet processes. A recent example is the calculation of the production rates of a W boson in association with up to five jets [5], performed using the BlackHat approach [6] to loop integrals calculations;
- the capability to evaluate loop integrals numerically has lead to the full automation of NLO calculations, from the generation of Feynman diagrams to the calculation itself, and on to its matching with PS Monte Carlos. The first implementations of this kind can be found in aMC@NLO [7], OpenLoops [8] and PowHel[3] [9]. This has led some people to declare that "NLO calculations are a solved problem";
- NNLO calculations, initially available only for a handful of simple processes like structure functions [10,11], inclusive vector boson [12,13] and inclusive Higgs boson hadroproduction [14–16], have started to become available for more differential distributions. Examples for Higgs boson productions are given in Refs. [17] and [18]. Calculations of more

[1] There are, however, important exceptions to this. The flavor-changing neutral current decay $b \to s\gamma$ and the production of a Higgs boson in gluon–gluon fusion, whose leading order perturbative terms are given by one-loop Feynman diagrams, are prime examples.

[2] This description of the state of the art, and what follows in this paper, mainly applies to processes related to hadroproduction of particles, whose calculations are particularly difficult because they are initiated by quarks and gluons and have complex final states. In other cases, for instance decay processes or evolution equations for masses in SuperSymmetry, the basic processes are simpler, and precise multi-loop calculations have been a standard much earlier than described here. A full description of the state of theoretical calculations in these two fields, which are of course as important as collider processes for searches of physics beyond the SM, would however require a separate article.

[3] This code is not yet public.

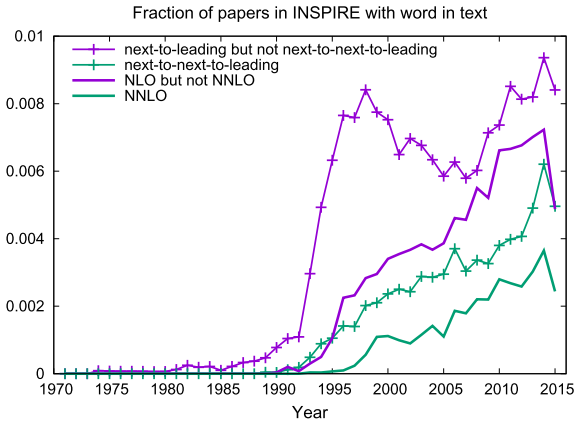

Fig. 1. (Color online.) Fraction of papers in INSPIRE (http://inspirehep.net/) containing the string "next-to-leading" but not "next-to-next-to-leading" (purple line with crosses) or containing the string 'next-to-next-to-leading' (green line with crosses) as a function of the year of publication. The same analysis done using instead the acronyms "NLO" and "NNLO" is also shown (lines without crosses).

complex processes have also recently started to appear. A few examples, chosen among the most relevant ones, are top–antitop pair production [19], dijet production [20], Higgs boson plus a jet [22,21];

- matching to parton shower Monte Carlos starts to be extended to NNLO accuracy. First results have appeared for Higgs boson production [23,24] and for the Drell–Yan process [25];
- the first results of an unprecedented NNNLO (also denoted as N^3LO) calculation of a hadroproduction process (Higgs boson in gluon fusion) have recently appeared [26].

The "advance" of NNLO calculations and a resurgence of the NLO ones in recently published papers, possibly related to the broad availability of automation, can be appreciated in Fig. 1, where the fraction of papers listed in INSPIRE containing respectively the string "next-to-leading" (but not "next-to-next-to-leading") and "next-to-next-to-leading" are plotted as a function of the year of publication. An alternative analysis, done using the acronyms NLO and NNLO instead, is also shown: the details vary, but the broad picture is the same.

It would be impossible to describe in detail in this review all the recent advances mentioned above, and even to cite all the papers that contributed to them. We shall therefore limit ourselves to give an example of the effect of higher-order corrections in one of today's most important processes, Higgs boson production via gluon fusion. The very recently completed NNNLO calculation [26] can be seen to have, at LHC energies, a theoretical uncertainty that can be as small as $^{+0.5}_{-3}\%$. This has to be compared with the $\pm$7–9% uncertainty of the NNLO calculation, and the $\pm$20% and $\pm$25% uncertainties of the NLO and LO results respectively. It is clear then that progress is being made, albeit slowly and at the price of many man-years work. On the other hand, increasing the precision of such calculations is mandatory if we hope to eventually observe small discrepancies between theory and measurements that may point to new physics beyond the Standard Model.

2. Inclusive cross-section measurements

For a cross-section measurement σ, experimentalists estimate the number of signal events S, which is the total number of selected events N minus the estimated number of background events B. This number is proportional to the product $\sigma \times L$ of the cross-section σ and the integrated luminosity L. The proportionality coefficient is the product $A \times \varepsilon$ of the analysis acceptance A and the detection efficiency ε. The parameter A, which is the extrapolation factor from the fiducial volume of the analysis to the full acceptance, is affected mostly by theoretical uncertainties due to model dependence. This is why measurements limited to the detector acceptance, called *fiducial* cross-section measurements, are often provided. The detection efficiency ε is itself the product of several efficiencies, from trigger, reconstruction and selection efficiencies. Whenever possible, these efficiencies are evaluated from the data themselves, presented as corrections to the efficiencies obtained from simulation, and therefore part of their uncertainties are statistical in nature.

The number of events from sources of backgrounds that cannot be obtained reliably from the simulation are extrapolated from signal-depleted regions of the phase space in the data (control samples) to the signal region. In the most sophisticated analysis techniques employed at the LHC, the signal extraction is performed in simultaneous fits to the final and control samples, to account correctly for correlations. Some of the backgrounds, for which good theoretical models exist, are estimated from the simulation. The detector simulations of LHC experiments, based on the GEANT-4 tool kit [27], are sophisticated and constantly improved. Most importantly, the data are used for alignment and calibration purposes, and to determine the energy and momentum scales of the various *objects* (photons, electrons, muons, tau leptons, jets, b-tagged jets, missing transverse momentum). Once corrected based on the data, simulations are used to determine signal efficiencies and detector resolutions, as well as to optimize the signal selection and background rejection. When it comes to detecting

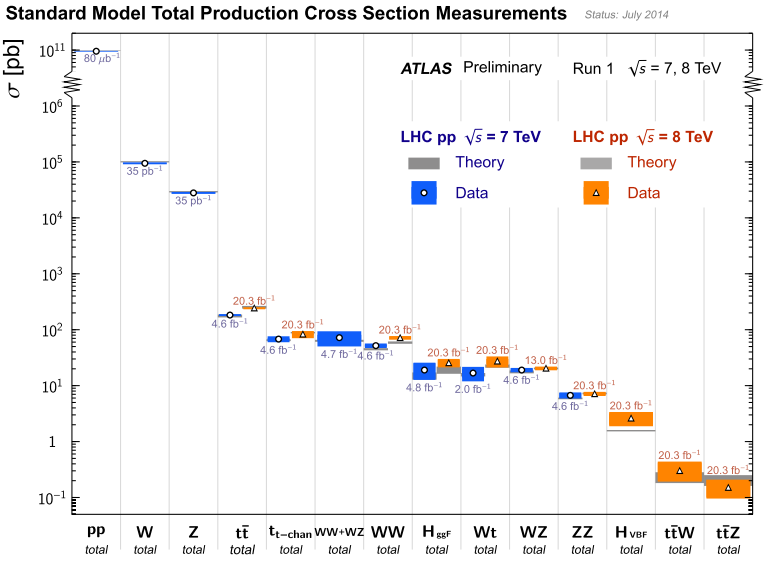

Fig. 2. (Color online.) Summary of inclusive cross section measurements at ATLAS.

very small signals in the context of large backgrounds, the LHC experiments often exploit the power of multivariate analyses (MVA) to improve background to signal discrimination.

The luminosity L is the integral of the instantaneous luminosity delivered by the LHC over the considered running period and is expressed in inverse-femtobarns fb^{-1}. During the Run-1 of the LHC, ATLAS [28] and CMS [29] have each recorded 5 fb^{-1} of data at a center of mass energy of 7 TeV in 2011 and 20 fb^{-1} at 8 TeV in 2012, and LHCb [30] has recorded 1 and 2 fb^{-1} at 7 and 8 TeV, respectively. The profile of instantaneous luminosity has changed a lot in the course of Run-1, from 3 to $8{\cdot}10^{33}$ $\text{cm}^{-2}{\cdot}\text{s}^{-1}$ in 2012. This translates into varying conditions of *pile-up*, from 10 to 25 hard proton–proton interactions in average per bunch crossing. The pile-up mitigation is one of the experimental challenges at the LHC, which has in particular motivated the development of particle flow techniques in ATLAS and CMS.

Many inclusive production cross-section have been measured at the LHC and compared to the SM predictions. Very nice agreement between measurements and predictions is observed, over a wide range of values, from the total inelastic proton–proton cross-section in the tens of mb range, the W and Z boson production in the tens of nb range, and the multi boson production in the tens of pb range. The smallest measured cross-sections are in the range of a tenth of a pb. In effect LHC measurements probe inclusive cross-sections over 12 orders of magnitude. This is illustrated for ATLAS [31] in Fig. 2 and similar agreement with predictions on inclusive cross-sections is reached at CMS [32]. This extended set of measurements in agreement with the predictions demonstrates the excellent understanding of both underlying SM physics and detectors.

2.1. Vector boson production

There is a strong interest for the physics of electroweak vector bosons at the LHC. Measurements of single W and Z boson productions is a way to test the left/right couplings of light quarks, to probe the quark and gluon contents of the proton (parton densities, or PDFs), to test higher-order QCD calculations in the associated production with jets.

The main W-boson signature is one prompt, energetic, isolated charged lepton (e, μ) plus a neutrino giving rise to missing transverse momentum $E_{\text{T}}^{\text{miss}}$. The lepton momentum and the $E_{\text{T}}^{\text{miss}}$ are combined to form the so-called transverse mass M_{T}, which is an observable with a characteristic Jacobian distribution (Fig. 3, left) from which the mass of the W boson can in principle be measured. The isolation criterion is necessary to discriminate against fake leptons and leptons produced in heavy-flavor hadron decays, which are most likely produced close to jet activity. The main Z-boson signature is a pair of same-flavor oppositely-charged prompt, energetic, isolated leptons originating from the same reconstructed proton–proton collision vertex and with an invariant mass around 91 GeV (Fig. 3-right). The leptons are reconstructed within the tracker, calorimeter and/or muon system acceptance, typically for $|\eta| < 2.5$ in ATLAS and CMS, and with p_{T} thresholds that are largely determined by trigger requirements, typically 30 GeV for single electron triggers, and 20 GeV for single muon triggers.[4]

[4] p_{T} denotes the component of a particle's momentum that is transverse to the beam axis, while p_z is the component parallel to the beams. We define the rapidity $y \equiv \frac{1}{2}\ln(E+p_z)/(E-p_z)$, where the energy E satisfies $E^2 = m^2 + p_{\text{T}}^2 + p_z^2$ and m is the particle's mass. We also define the pseudo-rapidity $\eta \equiv -\ln\tan\theta/2$, where θ is the angle of the momentum with respect to the beams. Pseudo-rapidity and rapidity coincide in the ultra-relativistic limit, $E \gg m$.

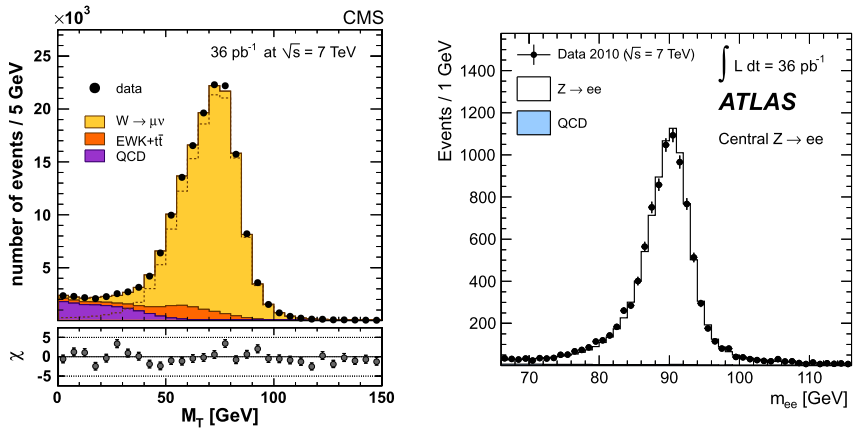

Fig. 3. (Color online.) Examples of early electroweak boson signals, obtained with the 2010 data at 7 TeV. On the left side, the transverse mass distribution in the $W \to \mu\nu$ channel in CMS. On the right side, the invariant mass distribution in the $Z \to e^+e^-$ channel in ATLAS.

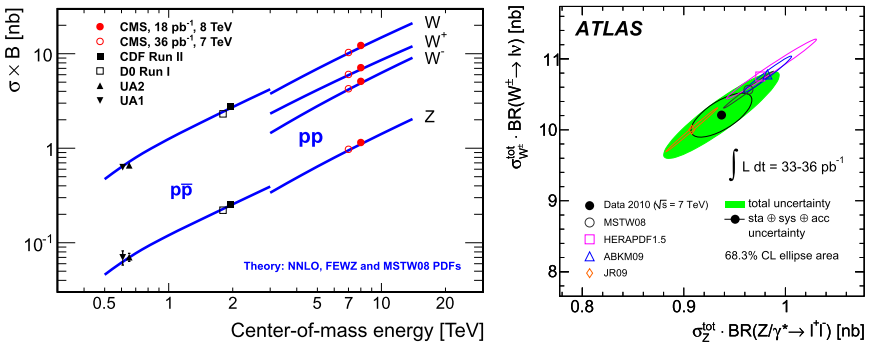

Fig. 4. (Color online.) On the left side, inclusive W and Z production cross-section times branching fractions in $p\bar{p}$ and pp collisions as a function of the collider's center of mass energy. The data points at 7 and 8 TeV are CMS measurements. On the right side, inclusive W versus Z production cross-sections times branching fractions in 7 TeV collisions at ATLAS, with predictions obtained using several PDF sets.

At 7/8 TeV, the inclusive W production cross-section is of the order of 100 pb, and three times less for the Z production. Taking into account leptonic branching fractions and typical detector acceptance and detection efficiency, this corresponds to approximately 5 million W events per lepton flavor and fb^{-1}, and ten times less Z events. These huge W and Z signals in leptonic decay modes are used as *standard candles* for trigger, calibration, detector modeling, alignment, energy scale and luminosity monitoring purposes. The three di-lepton narrow states, J/ψ, Υ and Z, are also used to assess the uniformity and linearity of the detector response. Processes involving vector bosons often constitute backgrounds in SM measurements, such as in top quark and Higgs boson measurements, or in BSM searches. Results for the inclusive cross-section measurements from ATLAS [33] and CMS [34,35] are shown on Fig. 4.

Compared to electrons and muons, τ leptons are more complicated to reconstruct due to multiple possible decay channels and the presence of at least one additional neutrino in the final state. Nevertheless electroweak bosons are also studied extensively at ATLAS and CMS in decay channels with τ leptons [36,37], mostly as a crucial validation of τ-lepton reconstruction and identification, which are important for Higgs boson studies and other searches. Hadronic decays of electroweak bosons are also exploited in regions of phase space where the huge QCD background is kinematically suppressed, for instance is multi-boson production studies. Recently techniques of reconstruction of highly boosted electroweak bosons giving rise to merged jets with jet substructures have been developed and are giving spectacular results [38].

3. Differential cross-section measurements

Differential cross-section measurements allow even more precise tests of the SM dynamics. Jets, photons, W and Z bosons, are studied either in single or multiple production. In single production, differential cross-sections are measured as a function of the production transverse momentum p_T or absolute rapidity y. For multiple production, cross-section measurements as a function of the invariant mass of the system or of angular variables, are also given.

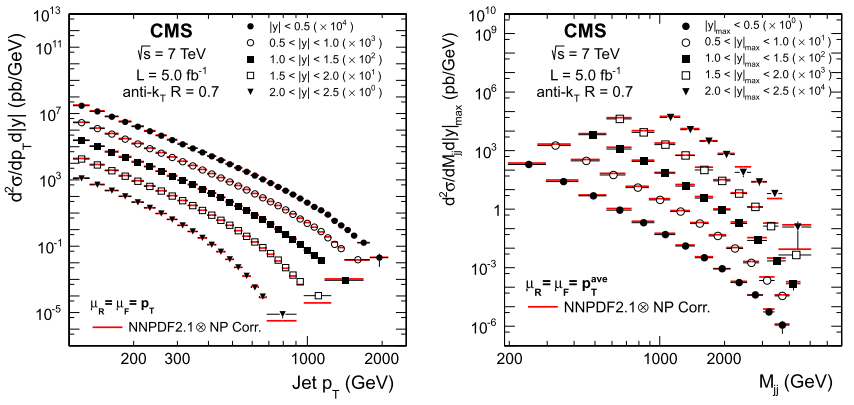

Fig. 5. (Color online.) Inclusive jet cross-section as a function transverse momentum (left) and di-jet mass spectrum (right) in five bins of absolute rapidity, for data (markers) and theory (thick red lines).

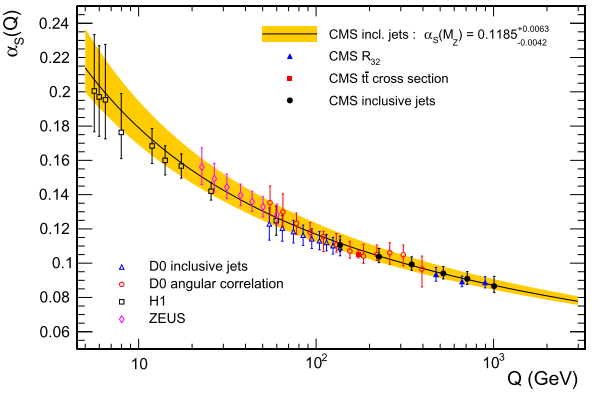

Fig. 6. (Color online.) The strong coupling α_S (solid line) as a function of the momentum transfer $Q = p_T$. Recent CMS jet results are shown and compared to results from H1, ZEUS and D0 experiments. These results are consistent with determinations at e^+e^- colliders, $\alpha_S(M_Z) = 0.1177 \pm 0.0046$ [41].

3.1. Jet and di-jet production

The jet cross-section measurements cover typically a phase space up to 2 TeV in jet transverse momentum and up to 3 in absolute jet rapidity [39,40]. The di-jet mass spectra extend typically up to 5 TeV. Fig. 5 presents p_T distributions of jets and the mass distribution of di-jets in various bins of the jet or di-jet absolute rapidity.

These and other jet-based data constrain the parton distribution functions of the proton, notably for the gluon at high fractions of the proton momentum, and provide input to determine the strong coupling at high momentum scales, as illustrated in Fig. 6. The high center-of-mass energy of the LHC allows for studying the scale dependence of the strong coupling constant up to unprecedented scale [42].

3.2. The Drell–Yan process

The production of lepton pairs through quark antiquark annihilation is known as the Drell–Yan (DY) process. This is the main W and Z production process studied at the LHC, which probes the valence quark and sea quark and antiquark content of the proton over a wide range of x and four-momentum transfer Q^2, in the region $x \sim 10^{-4}$ to 10^{-1} and $Q^2 \sim 5 \times 10^2$ to 10^6 GeV^2. An example of DY spectrum in the combined e^+e^- and $\mu^+\mu^-$ channels at 8 TeV by CMS [43] and in the e^+e^- channel at 7 TeV by ATLAS [44] are presented in Fig. 7. The measurements, performed as a function of the lepton pair invariant mass from 15 GeV to 1.5 TeV, and fully corrected for acceptance, detector efficiency and detector resolution, are compared to state-of-the-art theoretical calculations at the NNLO in QCD including electroweak corrections. A remarkable agreement is found over more than 8 orders of magnitude in cross-section.

Differential production cross-section measurements are important ancillary measurements for the eventual measurement of the W boson mass. The W and Z boson differential cross-sections as functions of boson transverse momentum q_T and rapidity have been measured at both 7 and 8 TeV. Fig. 8 presents the transverse momentum spectrum of Z bosons, fully corrected for acceptance and detector effects, based on 4.7 fb^{-1} of TeV data at ATLAS [45]. The bulk of electroweak boson production is found at relatively low q_T, where the predictions are delicate, whereas at high q_T the data are well-described

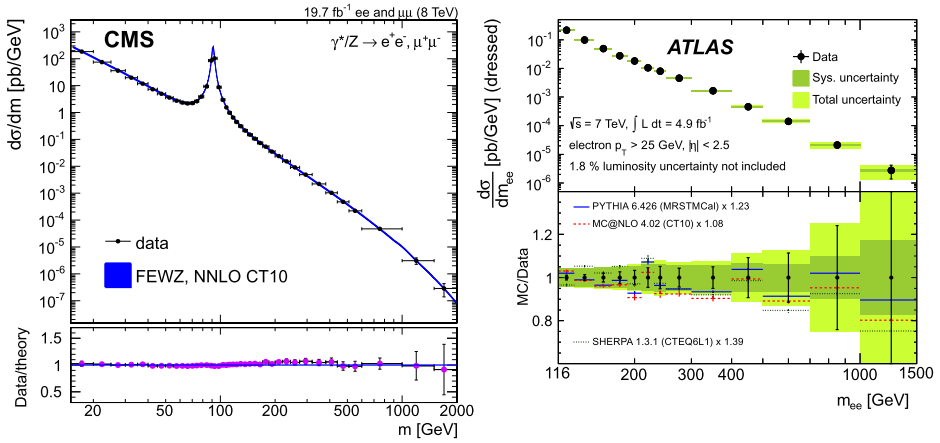

Fig. 7. (Color online.) The fully-corrected Drell–Yan spectrum in 8-TeV data, between 15 and 1500 GeV in electron and muon channels at CMS (left), and the uncorrected Drell–Yan spectrum in 7-TeV data between 116 and 1500 GeV in the electron channel at ATLAS, as measured and as predicted by calculations.

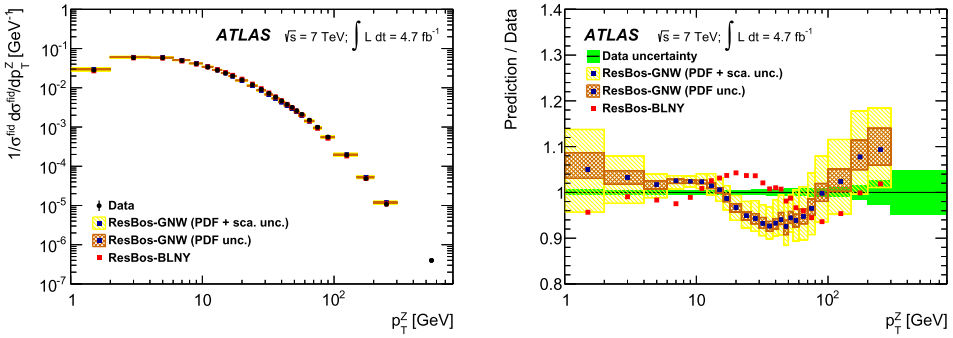

Fig. 8. (Color online.) The fully-corrected Z transverse momentum spectrum in 7-TeV data at ATLAS, as measured and as predicted by calculations, on the left, and ratio of various predictions to the data, on the right.

using NNLO perturbative calculations, here using RESBOS [46]. The rapidity y of the produced vector bosons is also important as being directly related to the momentum fractions of the initial partons.

3.3. Lepton charge asymmetry

At the LHC the rapidity plateau for electroweak boson production extends way beyond that at the Tevatron, up to $|y| = 3.5$. Interestingly, the LHC being a proton–proton collider, the rapidity distributions for the W^+ and W^- bosons are different, the dominant production processes being $u\bar{d} \to W^+$ and $d\bar{u} \to W^-$. As a result of the density of up valence quarks in protons at large x being larger than the density of down valence quarks, the rapidity plateau for the W^+ extends further than that of the W^-. Although it is in principle possible to reconstruct the rapidity of a W boson from the lepton momentum and the $E_{\mathrm{T}}^{\mathrm{miss}}$ using a W-mass constraint on the lepton–neutrino pair, the difference in rapidity distributions is usually studied by looking at the charge asymmetry of leptons from W decays as a function of pseudo-rapidity, which is an interplay of the density of valence and sea quarks in the proton and of the V–A structure of the W production and decay. Although the W charge asymmetry is positive at all rapidities, the lepton charge asymmetry is positive in the acceptance of ATLAS and CMS and changes sign in the acceptance of LHCb typically around $|\eta| \simeq 3$, depending on the lepton p_{T} threshold (see Fig. 9). These studies yield significant improvement on u, d and u/d quark PDFs in the range $10^{-3} < x < 10^{-2}$ [47,48]

3.4. Gauge bosons plus jets

The productions of gauge bosons in association with jets are extensively studied. Cross-sections that are measured up to seven jets span 5 orders of magnitude with respect to the inclusive production (Fig. 10), and good agreement with calculations and Monte Carlo models are found [49,50]. The dynamics of the jet production is also studied; this includes the transverse momentum and rapidity spectra of the jets as well as the various jet–jet and jet–boson angles. No model reproduces exactly all the features of these productions, but in general, fixed-order NLO calculations such as BLACKHAT+Sherpa [6] give better agreement with the data than Monte Carlo models.

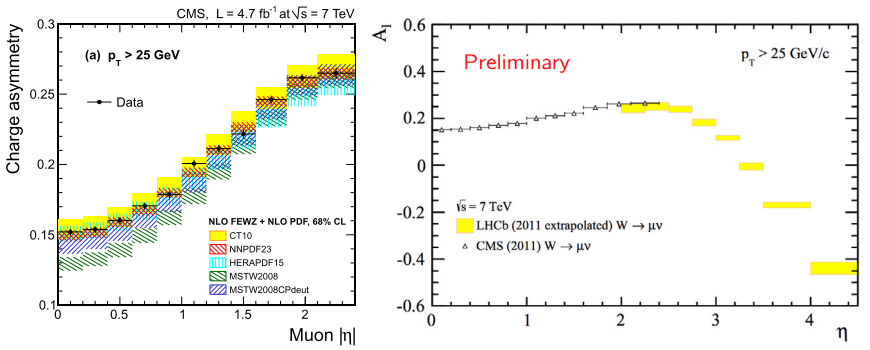

Fig. 9. (Color online.) Muon charge asymmetry as a function of absolute pseudo-rapidity η in 7-TeV data for a p_T threshold of 25 GeV, as measured by CMS on the left side, and by CMS and LHCb on the right side. The CMS points on the right-hand plot are identical to those presented on the left-hand plot, and the LHCb points are extrapolated to match the CMS threshold. On the left-hand plot, the CMS data points are compared to NLO predictions calculated using the FEWZ3.1 MC tool interfaced with various PDF sets. The acceptance of LHCb is complementary and allows one to extend the coverage of EW boson studies to the high-rapidity region and therefore to explore quark densities at lower x.

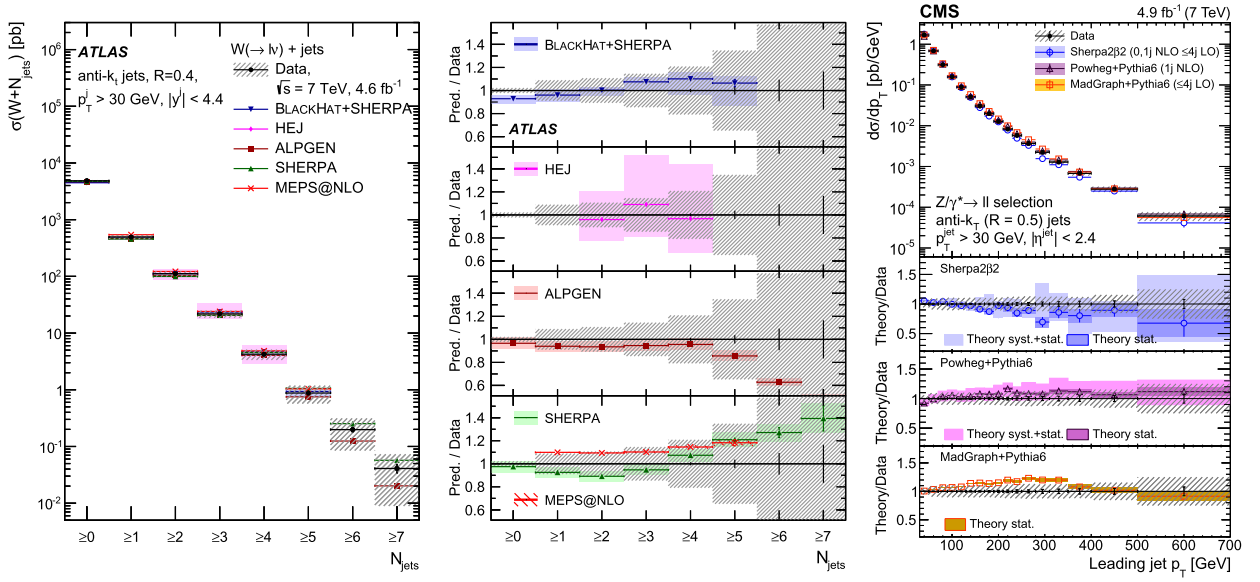

Fig. 10. (Color online.) Production of EW bosons in association with hadronic jets. On the left side is presented the distribution of the inclusive number of jets produced in association with a $W \to \ell\nu$ in 4.6 fb^{-1} of 7-TeV data at ATLAS and, on the middle panel, the comparison with various models. On the right side is shown the transverse momentum distribution of the leading jet in $Z \to \ell\ell + \geq 1$ jet events in 4.9 fb^{-1} of 7-TeV data at CMS, with comparisons with various models.

Associated production of W and Z bosons with heavy flavors (c and b quarks) is performed to constraint the s, c and b quark densities in the proton. This programme is crucial to understand how to convert the well-measured Z q_T distribution into a prediction for the W q_T distribution, which can in turn be used to reduce the systematic uncertainties on the ultimate measurement of the W boson mass.

3.5. Forward–backward asymmetry of lepton pairs

Measurement of the forward–backward asymmetry A_{FB} in Z boson production is complicated at the LHC due to the symmetric proton–proton initial state. However, because the longitudinal momentum fraction carried out by valence quarks is larger in average, there is a correlation between the rapidity of the produced Z boson and the direction of the initial-state quark that can be exploited to measure the effective weak mixing angle. Both CMS [51] and ATLAS [52] have produced differential measurements of A_{FB} as a function of the dilepton invariant mass, see Fig. 11, left. These measurements are not as precise as at LEP, but allow us to probe the scale dependence of the electro-weak interactions up to unprecedented scales of the order of 400 GeV. The study of A_{FB} at high invariant mass is also a sensitive probe of the presence of new massive gauge bosons.

Direct measurements of the effective weak mixing angle can also be performed at the Z pole, but these are affected by the knowledge of the proton structure and by the limited acceptance of the experiments [53]. Recently, by exploiting the

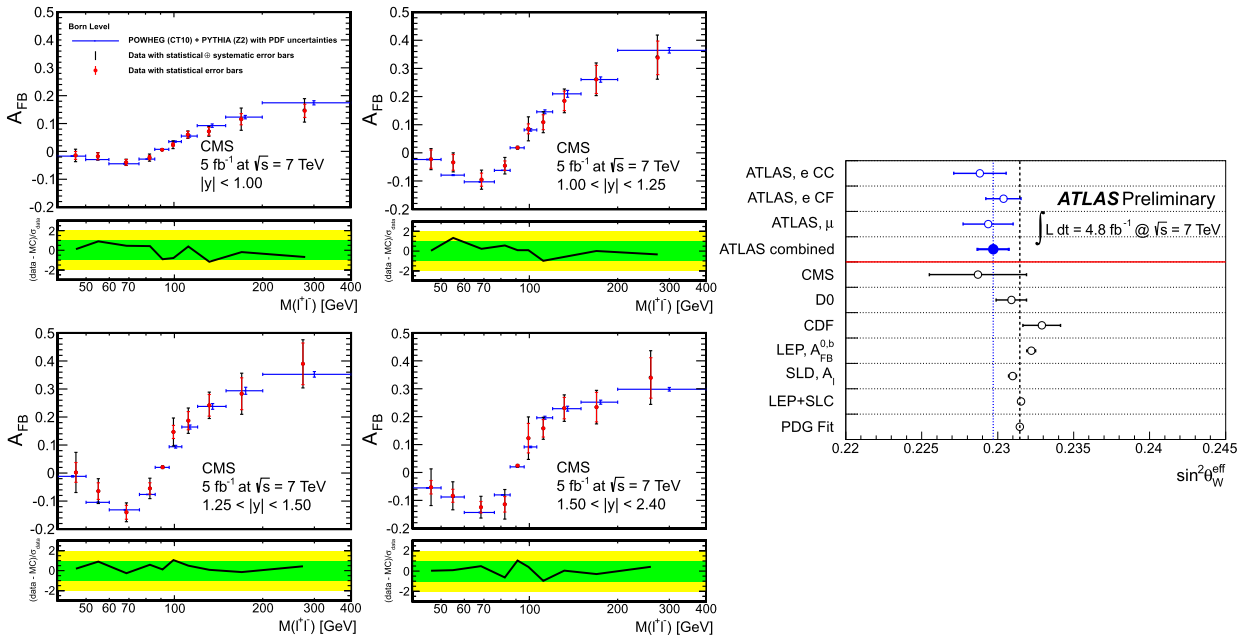

Fig. 11. (Color online.) On the left side, measurement of A_{FB} in four region of the dilepton rapidity, as a function of the dilepton invariant mass, corrected from detector resolution effects and for final state radiation. The lepton asymmetry is measured in the Collins–Soper frame under the assumption that the initial-state parton with the smaller momentum fraction is the anti-quark. The agreement with theory prediction is good. On the right side, comparison of the preliminary measurement of $\sin^2\theta_{\mathrm{W}}^{\mathrm{eff}}$ at ATLAS with previous measurements at CMS, and at Tevatron and SLC/LEP experiments.

detection of electrons in the forward calorimetry, ATLAS has produced the most precise measurement at the LHC [52], see Fig. 11, right.

4. Multi-boson production

The high energy at the LHC gives access to the production of multi bosons as a way to test directly the gauge structure of the electroweak theory.

In the SM, only the $W^+W^-\gamma$ and W^+W^-Z vertices occur as triple couplings; all other vertices involve anomalous triple gauge couplings (aTGC), in particular those involving three neutral bosons, which are forbidden by Bose symmetry. The aTGCs can be probed experimentally by studying the pair production of gauge bosons via quark–antiquark annihilation ($q\bar{q}$). The most advanced constraints on aTGCs are obtained by the analysis of diboson final states, $W^{\pm}\gamma$, $Z\gamma$, W^+W^-, $W^{\pm}Z$, ZZ. This extensive program is on-going: most of the modes have been measured at 7 TeV [54–57] and some of them (mostly those constituting irreducible backgrounds for Higgs boson studies) at 8 TeV [58]. The contribution of aTGCs in diboson production can in general be isolated where the outgoing bosons have very high transverse momenta or where the pair has a very high invariant mass, but so far no significant deviations have been reported. Another way to probe triple gauge coupling is to look for the electroweak production of gauge bosons via vector boson fusion (VBF); these are very small signals and among the smallest production cross-sections measured at the LHC [59,60].

The quartic gauge couplings can be experimentally probed by investigating triboson production and diboson production via VBF. This important field of research is just beginning, and first signals, consistent with SM predictions, are observed [61–63].

5. Conclusion

In this article we have presented examples of theoretical calculations and measurements by LHC experiments in the field of strong and electroweak interactions. So far, all the measurements are in good agreement with the most recent theory predictions. First examples of calculations that go beyond NNLO have started to appear, namely for the flagship process of Higgs boson production in gluon-fusion. The data allow for an improved knowledge of the quark and gluon densities in the proton in regions of phase space that are relevant for predictions of Higgs boson, SUSY and BSM signals at the LHC. The running of the strong coupling constant is verified up to the TeV scale. The production of W and Z bosons at the LHC is being studied in great detail, as is necessary for the eventual precise determination of the mass of the W boson. The triple and, more recently, quartic gauge couplings are being probed; no significant deviation is found in the gauge sector. The multiple production of gauge bosons in association with high-rapidity jets, which will eventually allow us to explore the restoration of unitarity in boson scattering at high energy, a process of the heart of electroweak symmetry breaking, has

begun and will continue in the coming years, at the higher collider energies of 13 or 14 TeV, with ten times, and possibly a hundred times, more data.

References

[1] ATLAS Collaboration, Observation of a new particle in the search for the Standard Model Higgs boson with the ATLAS detector at the LHC, Phys. Lett. B 716 (2012) 1, arXiv:1207.7214 [hep-ex].
[2] CMS Collaboration, Observation of a new boson at a mass of 125 GeV with the CMS experiment at the LHC, Phys. Lett. B 716 (2012) 30, arXiv:1207.7235 [hep-ex].
[3] S. Frixione, B.R. Webber, Matching NLO QCD computations and parton shower simulations, J. High Energy Phys. 0206 (2002) 029, arXiv:hep-ph/0204244.
[4] P. Nason, A new method for combining NLO QCD with shower Monte Carlo algorithms, J. High Energy Phys. 0411 (2004) 040, arXiv:hep-ph/0409146.
[5] Z. Bern, L. Dixon, F. Febres Cordero, S. Hoeche, H. Ita, et al., Next-to-leading order $W + 5$-jet production at the LHC, Phys. Rev. D 88 (2013) 014025, arXiv:1304.1253 [hep-ph].
[6] C. Berger, Z. Bern, L. Dixon, F. Febres Cordero, D. Forde, et al., An automated implementation of on-shell methods for one-loop amplitudes, Phys. Rev. D 78 (2008) 036003, arXiv:0803.4180 [hep-ph].
[7] J. Alwall, R. Frederix, S. Frixione, V. Hirschi, F. Maltoni, et al., The automated computation of tree-level and next-to-leading order differential cross sections, and their matching to parton shower simulations, J. High Energy Phys. 1407 (2014) 079, arXiv:1405.0301 [hep-ph].
[8] F. Cascioli, P. Maierhofer, S. Pozzorini, Scattering amplitudes with open loops, Phys. Rev. Lett. 108 (2012) 111601, arXiv:1111.5206 [hep-ph].
[9] M. Garzelli, A. Kardos, Z. Trocsanyi, NLO event samples for the LHC, PoS EPS-HEP2011 (2011) 282, arXiv:1111.1446 [hep-ph].
[10] E. Zijlstra, W. van Neerven, Order α_s^2 QCD corrections to the deep inelastic proton structure functions F_2 and F_L, Nucl. Phys. B 383 (1992) 525–574.
[11] E. Zijlstra, W. van Neerven, Order α_s^2 correction to the structure function $F_3(x, Q^2)$ in deep inelastic neutrino-hadron scattering, Phys. Lett. B 297 (1992) 377–384.
[12] R. Hamberg, W. van Neerven, T. Matsuura, A complete calculation of the order α_s^2 correction to the Drell–Yan K factor, Nucl. Phys. B 359 (1991) 343–405;
R. Hamberg, W. van Neerven, T. Matsuura, Nucl. Phys. B 644 (2002) 403–404 (Erratum).
[13] W. van Neerven, E. Zijlstra, The $\mathcal{O}(\alpha_s^2)$ corrected Drell–Yan K factor in the DIS and MS scheme, Nucl. Phys. B 382 (1992) 11–62;
W. van Neerven, E. Zijlstra, Nucl. Phys. B 680 (2004) 513–514 (Erratum).
[14] R.V. Harlander, W.B. Kilgore, Next-to-next-to-leading order Higgs production at hadron colliders, Phys. Rev. Lett. 88 (2002) 201801, arXiv:hep-ph/0201206.
[15] C. Anastasiou, K. Melnikov, Higgs boson production at hadron colliders in NNLO QCD, Nucl. Phys. B 646 (2002) 220–256, arXiv:hep-ph/0207004.
[16] V. Ravindran, J. Smith, W.L. van Neerven, NNLO corrections to the total cross-section for Higgs boson production in hadron–hadron collisions, Nucl. Phys. B 665 (2003) 325–366, arXiv:hep-ph/0302135.
[17] C. Anastasiou, K. Melnikov, F. Petriello, Fully differential Higgs boson production and the di-photon signal through next-to-next-to-leading order, Nucl. Phys. B 724 (2005) 197–246, arXiv:hep-ph/0501130.
[18] S. Catani, M. Grazzini, An NNLO subtraction formalism in hadron collisions and its application to Higgs boson production at the LHC, Phys. Rev. Lett. 98 (2007) 222002, arXiv:hep-ph/0703012.
[19] M. Czakon, P. Fiedler, A. Mitov, Total top-quark pair-production cross section at hadron colliders through $\mathcal{O}(\alpha_s^4)$, Phys. Rev. Lett. 110 (2013) 252004, arXiv:1303.6254 [hep-ph].
[20] A. Gehrmann-De Ridder, T. Gehrmann, E. Glover, J. Pires, Second order QCD corrections to jet production at hadron colliders: the all-gluon contribution, Phys. Rev. Lett. 110 (16) (2013) 162003, arXiv:1301.7310 [hep-ph].
[21] X. Chen, T. Gehrmann, E. Glover, M. Jaquier, Precise QCD predictions for the production of Higgs + jet final states, Phys. Lett. B 740 (2015) 147–150, arXiv:1408.5325 [hep-ph].
[22] R. Boughezal, F. Caola, K. Melnikov, F. Petriello, M. Schulze, Higgs boson production in association with a jet at next-to-next-to-leading order in perturbative QCD, J. High Energy Phys. 1306 (2013) 072, arXiv:1302.6216 [hep-ph].
[23] K. Hamilton, P. Nason, E. Re, G. Zanderighi, NNLOPS simulation of Higgs boson production, J. High Energy Phys. 1310 (2013) 222, arXiv:1309.0017 [hep-ph].
[24] S. Hoeche, Y. Li, S. Prestel, Higgs-boson production through gluon fusion at NNLO QCD with parton showers, Phys. Rev. D 90 (5) (2014) 054011, arXiv:1407.3773 [hep-ph].
[25] A. Karlberg, E. Re, G. Zanderighi, NNLOPS accurate Drell–Yan production, J. High Energy Phys. 1409 (2014) 134, arXiv:1407.2940 [hep-ph].
[26] C. Anastasiou, C. Duhr, F. Dulat, F. Herzog, B. Mistlberger, Higgs boson gluon-fusion production in $\mathrm{N^3LO}$ QCD, arXiv:1503.06056 [hep-ph].
[27] GEANT4 Collaboration, S. Agostinelli, et al., GEANT4: a simulation toolkit, Nucl. Instrum. Methods A 506 (2003) 250–303.
[28] ATLAS Collaboration, The ATLAS experiment at the CERN large hadron collider, J. Instrum. 3 (2008) S08003.
[29] CMS Collaboration, The CMS experiment at the CERN large hadron collider, J. Instrum. 3 (2008) S08004.
[30] LHCb Collaboration, The LHCb detector at the LHC, J. Instrum. 3 (2008) S08005.
[31] ATLAS Collaboration, ATLAS standard model public results, CERN, https://twiki.cern.ch/twiki/bin/view/AtlasPublic/StandardModelPublicResults.
[32] CMS Collaboration, CMS standard model public results, CERN, https://twiki.cern.ch/twiki/bin/view/CMSPublic/PhysicsResultsSMP.
[33] ATLAS Collaboration, Measurement of the inclusive $W^{\pm}$ and Z/γ cross sections in the electron and muon decay channels in pp collisions at $\sqrt{s} =$ 7 TeV with the ATLAS detector, Phys. Rev. D 85 (2012) 072004, arXiv:1109.5141 [hep-ex].
[34] CMS Collaboration, Measurement of the inclusive W and Z production cross sections in pp collisions at $\sqrt{s} = 7$ TeV, J. High Energy Phys. 1110 (2011) 132, arXiv:1107.4789 [hep-ex].
[35] CMS Collaboration, Measurement of inclusive W and Z boson production cross sections in pp collisions at $\sqrt{s} = 8$ TeV, Phys. Rev. Lett. 112 (2014) 191802, arXiv:1402.0923 [hep-ex].
[36] ATLAS Collaboration, Measurement of the W to $\tau\nu$ cross section in pp collisions at $\sqrt{s} = 7$ TeV with the ATLAS experiment, Phys. Lett. B 706 (2012) 276–294, arXiv:1108.4101 [hep-ex].
[37] CMS Collaboration, Measurement of the inclusive Z cross section via decays to τ pairs in pp collisions at $\sqrt{s} = 7$ TeV, J. High Energy Phys. 1108 (2011) 117, arXiv:1104.1617 [hep-ex].
[38] ATLAS Collaboration, Measurement of the cross-section of high transverse momentum vector bosons reconstructed as single jets and studies of jet substructure in pp collisions at $\sqrt{s} = 7$ TeV with the ATLAS detector, New J. Phys. 16 (2014) 113013, arXiv:1407.0800 [hep-ex].
[39] ATLAS Collaboration, Measurement of the inclusive jet cross-section in proton–proton collisions at $\sqrt{s} = 7$ TeV using 4.5 fb^{-1} of data with the ATLAS detector, arXiv:1410.8857 [hep-ex].
[40] CMS Collaboration, Measurements of differential jet cross sections in proton–proton collisions at $\sqrt{s} = 7$ TeV with the CMS detector, Phys. Rev. D 87 (2013) 112002, arXiv:1212.6660 [hep-ex].

[41] Particle Data Group Collaboration, K. Olive, et al., Review of particle physics, Chin. Phys. C 38 (2014) 090001.
[42] CMS Collaboration, Constraints on parton distribution functions and extraction of the strong coupling constant from the inclusive jet cross section in pp collisions at $\sqrt{s} = 7$ TeV, arXiv:1410.6765 [hep-ex].
[43] CMS Collaboration, Measurements of differential and double-differential Drell–Yan cross sections in proton–proton collisions at 8 TeV, arXiv:1412.1115 [hep-ex].
[44] ATLAS Collaboration, Measurement of the high-mass Drell–Yan differential cross-section in pp collisions at $\sqrt{s} = 7$ TeV with the ATLAS detector, Phys. Lett. B 725 (2013) 223–242, arXiv:1305.4192 [hep-ex].
[45] ATLAS Collaboration, Measurement of the Z/γ^* boson transverse momentum distribution in pp collisions at $\sqrt{s} = 7$ TeV with the ATLAS detector, J. High Energy Phys. 1409 (2014) 145, arXiv:1406.3660 [hep-ex].
[46] C. Balazs, C. Yuan, Soft gluon effects on lepton pairs at hadron colliders, Phys. Rev. D 56 (1997) 5558–5583, arXiv:hep-ph/9704258.
[47] CMS Collaboration, Measurement of the muon charge asymmetry in inclusive $pp \to W + X$ production at $\sqrt{s} = 7$ TeV and an improved determination of light parton distribution functions, Phys. Rev. D 90 (2014) 032004, arXiv:1312.6283 [hep-ex].
[48] LHCb Collaboration, Measurement of the forward W boson cross-section in pp collisions at $\sqrt{s} = 7$ TeV, J. High Energy Phys. 12 (2014) 079, arXiv:1408.4354 [hep-ex].
[49] ATLAS Collaboration, Measurements of the W production cross sections in association with jets with the ATLAS detector, arXiv:1409.8639 [hep-ex].
[50] CMS Collaboration, Measurements of jet multiplicity and differential production cross sections of Z+jets events in proton–proton collisions at $\sqrt{s} =$ 7 TeV, arXiv:1408.3104 [hep-ex].
[51] CMS Collaboration, Forward–backward asymmetry of Drell–Yan lepton pairs in pp collisions at $\sqrt{s} = 7$ TeV, Phys. Lett. B 718 (2013) 752–772, arXiv:1207.3973 [hep-ex].
[52] ATLAS Collaboration, Measurement of the forward–backward asymmetry of Z/γ^* bosons decaying into electron and muon pairs with the ATLAS detector at $\sqrt{s} = 7$ TeV, 2013, ATLAS-CONF-2013-043.
[53] CMS Collaboration, Measurement of the weak mixing angle with the Drell–Yan process in proton–proton collisions at the LHC, Phys. Rev. D 84 (2011) 112002, arXiv:1110.2682 [hep-ex].
[54] ATLAS Collaboration, Measurements of $W\gamma$ and $Z\gamma$ production in pp collisions at $\sqrt{s} = 7$ TeV with the ATLAS detector at the LHC, Phys. Rev. D 87 (11) (2013) 112003, arXiv:1302.1283 [hep-ex].
[55] ATLAS Collaboration, Measurement of W^+W^- production in pp collisions at $\sqrt{s} = 7$ TeV with the ATLAS detector and limits on anomalous WWZ and $WW\gamma$ couplings, Phys. Rev. D 87 (11) (2013) 112001, arXiv:1210.2979 [hep-ex].
[56] ATLAS Collaboration, Measurement of ZZ production in pp collisions at $\sqrt{s} = 7$ TeV and limits on anomalous ZZZ and $ZZ\gamma$ couplings with the ATLAS detector, J. High Energy Phys. 1303 (2013) 128, arXiv:1211.6096 [hep-ex].
[57] ATLAS Collaboration, Measurement of WZ production in proton–proton collisions at $\sqrt{s} = 7$ TeV with the ATLAS detector, Eur. Phys. J. C 72 (2012) 2173, arXiv:1208.1390 [hep-ex].
[58] CMS Collaboration, Measurement of the pp to ZZ production cross section and constraints on anomalous triple gauge couplings in four-lepton final states at $\sqrt{s} = 8$ TeV, Phys. Lett. B 740 (2015) 250, arXiv:1406.0113 [hep-ex].
[59] ATLAS Collaboration, Measurement of the electroweak production of dijets in association with a Z-boson and distributions sensitive to vector boson fusion in proton–proton collisions at $\sqrt{s} = 8$ TeV using the ATLAS detector, J. High Energy Phys. 1404 (2014) 031, arXiv:1401.7610 [hep-ex].
[60] CMS Collaboration, Measurement of the hadronic activity in events with a Z and two jets and extraction of the cross section for the electroweak production of a Z with two jets in pp collisions at $\sqrt{s} = 7$ TeV, J. High Energy Phys. 1310 (2013) 062, arXiv:1305.7389 [hep-ex].
[61] ATLAS Collaboration, Evidence for electroweak production of $W^\pm W^\pm jj$ in pp collisions at $\sqrt{s} = 8$ TeV with the ATLAS detector, Phys. Rev. Lett. 113 (14) (2014) 141803, arXiv:1405.6241 [hep-ex].
[62] CMS Collaboration, Search for $WW\gamma$ and $WZ\gamma$ production and constraints on anomalous quartic gauge couplings in pp collisions at $\sqrt{s} = 8$ TeV, Phys. Rev. D 90 (2014) 032008, arXiv:1404.4619 [hep-ex].
[63] CMS Collaboration, Study of exclusive two-photon production of W^+W^- in pp collisions at $\sqrt{s} = 7$ TeV and constraints on anomalous quartic gauge couplings, J. High Energy Phys. 1307 (2013) 116, arXiv:1305.5596 [hep-ex].